

Analyst

Accepted Manuscript



This is an *Accepted Manuscript*, which has been through the Royal Society of Chemistry peer review process and has been accepted for publication.

Accepted Manuscripts are published online shortly after acceptance, before technical editing, formatting and proof reading. Using this free service, authors can make their results available to the community, in citable form, before we publish the edited article. We will replace this *Accepted Manuscript* with the edited and formatted *Advance Article* as soon as it is available.

You can find more information about *Accepted Manuscripts* in the [Information for Authors](#).

Please note that technical editing may introduce minor changes to the text and/or graphics, which may alter content. The journal's standard [Terms & Conditions](#) and the [Ethical guidelines](#) still apply. In no event shall the Royal Society of Chemistry be held responsible for any errors or omissions in this *Accepted Manuscript* or any consequences arising from the use of any information it contains.

Evaluation of agglutination strength by flow-induced cell movement assay based surface plasmon resonance (SPR) technique[†]

Cite this: DOI: 10.1039/x0xx00000x

Krisda Sudprasert,^{a,b} Patjaree Peungthum,^{a,b} Apirom Vongsakulyanon,^f Ratthasart Amarith,^d Armote Somboonkaew,^d Boonsong Sutapun,^e Pimpun Kitpoka,^f Mongkol Kunakorn,^f Toemsak Srihirin^{a,b,c*}

Received 00th January 2012,
Accepted 00th January 2012

DOI: 10.1039/x0xx00000x

www.rsc.org/

A flow-induced cell movement assay combined with a surface plasmon resonance (SPR) technique was developed to quantify the agglutination strength, derived from the standard tube-agglutination test. Red blood cells (RBCs), based on the ABO blood group system, were specifically captured by anti-A and/or anti-B antibodies immobilized on a sensor surface. The agglutination strength corresponds to the amount of antigen–antibody interaction or the strength of RBC adhesion. Under a shear flow, the adherent RBCs were forced to move out of the region of interest with different average cell velocities (v_c) depending upon the adhesion strength and wall shear stress (WSS). Namely, a higher adhesion strength (higher agglutination strength) or lower WSS represents a lower v_c or vice versa. In this work, the agglutination strength was derived from the v_c that was calculated from the time derivative of the relative SPR signal by using a simple model of cell movement response, whose validity was verified. The v_c values of different samples were correlated with their agglutination strengths at a given WSS and antibody surface density. The v_c decreased as the agglutination strength increased, which can be considered as a linear regression. The coefficient of variation of the calculated v_c decreased to 0.1 as v_c increased to 30 $\mu\text{m}/\text{min}$. The sensitivity of this assay can be controlled by optimizing the antibody surface density or the WSS. This assay has the capability to resolve the antigen density of A₁ and B RBCs from that of A₁B RBCs.

Introduction

Human red blood cells (RBCs) are categorized into a blood group system based on the presence of antigen types on the RBC membrane.¹ The ABO blood group, composed of A antigens and B antigens, is the first and foremost system to consider before transfusion, because ABO-incompatible transfusion can be fatal.² The RBCs can be classified into four groups: A, B, AB, and O, and can be further divided into a subgroup system depending on the amount of antigens expressed on the RBCs; for example, subgroup A₁ > A₂ > A₃ or B > B₃.¹ The agglutination test is a standard technique for identifying blood group. By incubating unknown RBCs with known antibodies in solution phase or vice versa, the clumping of RBCs, mediated by crosslinking of the antigen–antibody binding, appears as a large complex. The strength of

agglutination, including 1+, 2+, 3+, and 4+ levels, is determined from the level of the agglutination form as seen by the naked eye. No agglutination due to an absence of antigen–antibody reaction is represented by 0.³ The agglutination strength relates directly to the amount of antigen–antibody binding, which normally depends on the antigen density on the RBCs. These levels must be sufficient to cover all subgroups to prevent false diagnosis. For example, 4+ strength is always the A₁ and B subgroup but a mixed field of 2–3+ strength can be found the A₃ or B₃ subgroup.

The surface plasmon resonance (SPR) technique was employed to measure biomolecular interaction, such as protein,⁴ DNA,^{5–7} and cellular detection⁸ in real time and without label molecules. Adsorption of analytes on a sensor surface can be monitored with high sensitivity via changes in the refractive index compared to a background. The SPR imaging technique, also known as SPR microscopy, has been developed for cellular studies such as detection of a target cell specifically binding to the sensor surface or cell-based assays investigating cell response under an external stimulus.⁸ When combined with microarray technology, SPR imaging is well regarded as a useful tool for high-throughput and multiplex analysis.^{9, 10} These capabilities confer advantages for the reduction of assay cost, detection time, and sample consumption. Therefore, the idea of applying the SPR technique to blood grouping is of interest. The first ABO blood grouping by using the SPR technique was reported.¹¹ The identification of the ABO blood group by using the specific antibody surfaces was successfully carried out and the antibody surface could be regenerated for repeated use. Hounkanghang *et al.* used SPR imaging in ABO blood

^aCenter of Intelligent Materials and Systems, Nanotec Center of Excellence at Mahidol University

^bMaterials Science and Engineering Programme, Faculty of Science, Mahidol University, Rama VI Rd., Phayathai, Bangkok, 10400, Thailand

^cDepartment of Physics, Faculty of Science, Mahidol University, Rama VI Rd., Phayathai, Bangkok, 10400, Thailand

^dPhotonics Technology Laboratory, National Electronics and Computer Technology Center (NECTEC), Pathumthani 12120, Thailand

^eSchool of telecommunication engineering, institute of engineering, Suranaree University of Technology, Muang, Nakhon Ratchasima, 30000, Thailand

^fDepartment of Pathology, Faculty of Medicine, Ramathibodi Hospital, Mahidol University, Rama VI Rd., Phayathai, Bangkok, 10400, Thailand

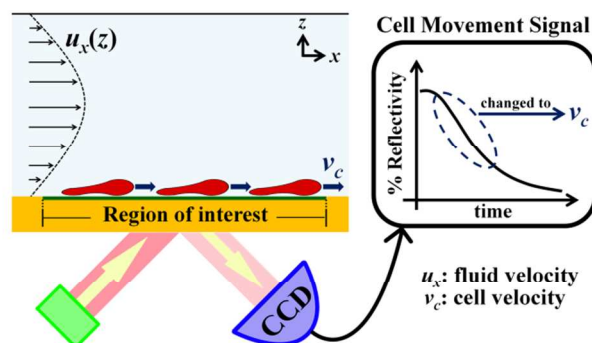
[†]Electronic Supplementary Information (ESI) available: See DOI: 10.1039/b000000x/

grouping for multiplex analysis, which could reduce the cost and analysis time.¹² However, to fully realize the SPR application for blood grouping, additional information on agglutination strength is needed.

Because RBC–RBC adhesion (the RBC agglutination) is based on the same principle as the adherence of RBCs on a surface, solid-phase biosensors such as the SPR technique can quantify the agglutination strength through the strength of cell–surface adhesion. A simple and standard method for quantitative analysis of the adhesion strength was determined by applying a fluid shear stress acting on the adherent cell.^{13, 14} This shear stress gives rise to the distraction of cell–surface binding, leading to detachment of cells from the surface. The adhesion strength was defined as the critical wall shear stress (critical WSS) at which 50% of the cell population remained.^{15, 16} To find out this critical WSS, the remaining RBCs under various WSSs (shear stress at a wall channel) have to be determined for a long time. Therefore, it is not suitable in real applications for blood grouping.

In general, the adherent RBCs under a given WSS below the critical WSS are moved by rolling along the surfaces without detaching.¹⁷ A kinetic model of the membrane–surface adhesion and its detachment under tension describing this phenomenon was proposed by Dembo *et al.* Based on the cell membrane–surface attachment mediated by receptors–ligand binding, an increase in the adhesion strength corresponds to increases in the ligand density on the surface, the receptor density on the cell membrane, and the ligand–receptor affinity, which are inversely proportional to the rolling velocity of the cell.¹⁸ This model was also used to describe rolling of adherent neutrophils mediated by selectin.¹⁹ Brunk *et al.* investigated sialyl Lewis^x-coated microspheres rolling along with the E-selectin surface under a shear flow. The relationship between the adhesion strength and the rolling velocity is described by a power function where the adhesion strength is inversely proportional to the velocity.²⁰ Therefore, we propose an average cell velocity (v_c , average velocity of the RBCs moving on the surface) to quantitatively evaluate the agglutination strength within a reasonable detection time.²¹ By fixing the WSS and finding v_c instead of the critical WSS, the assay time and the complication of adhesion strength analysis are reduced compared to the conventional method. However, based on the SPR technique, calibration between v_c and the adhesion strength or the agglutination strength is required.

In this work, the SPR technique together with a flow-induced cell movement assay was developed for evaluating the agglutination strength by monitoring v_c . The flow-induced cell movement assay was based on applying the WSS driving RBCs specifically adhering on a sensor surface which was immobilized by anti-A and/or anti-B antibody (Scheme 1). The SPR signal was converted to v_c by using a simple model of cell movement response, whose validity was also verified. The v_c , calculated from the SPR, was investigated in various conditions, including different densities of antibody surfaces and RBCs having different agglutination strengths. Finally, qualitative analysis of antigen density on the RBCs was exemplified and the precision of this assay was shown.



Scheme 1 Illustration of the flow-induced cell movement assay.

Experimental

Materials

SPR bare gold chips (50 nm of gold) coated on BK7 were purchased from Ssens (Netherlands). Dextran with a molecular weight of 500 kDa was purchased from Pharmacosmos A/S (Denmark). 1-ethyl-3-(3-diethyl-aminopropyl) carbodiimide (EDC), N-hydroxysuccinimide (NHS), glycerol, and ethanolamine were purchased from Sigma-Aldrich Co. (USA). Tween 20 (polyoxyethylene(20) sorbitan) was purchased from Merck KGaA (Germany). Pluronic F-127 and StabilCoat® immunoassay stabilizer were purchased from Sigma-Aldrich (Singapore). A flow cell made of polydimethylsiloxane (PDMS) was purchased from Dow Corning Co. (USA). IgM antibodies of the ABO blood system, including anti-A and anti-B, were obtained from the Thai Red Cross Society (Thailand). Deionized water (DI water) was used to prepare all aqueous solutions, including phosphate buffered solution (PBS: 0.15M NaCl, 0.01M phosphate, pH 7.4), normal saline solution (NSS: 0.9% NaCl (w/v)), glycerol, Pluronic F-127, and NaOH solution. All samples, used in this work, were left-over blood samples obtained from blood donors in the Blood Bank of Ramathibodi Hospital (Bangkok, Thailand) and they were typed for the ABO blood group by the standard agglutination technique. This work was approved by the Ramathibodi Hospital Ethics Committee.

Sample preparation

RBC samples were prepared from fresh Ethylenediaminetetraacetic acid (EDTA) blood. The EDTA blood was centrifuged at 3000 rpm for 1 minute. The blood components were separated into three layers consisting of the upper layer (plasma), the thin-middle layer (platelet and white blood cell), and the lower layer (RBC). The upper and middle layers were removed. The remaining RBCs were washed three times with NSS. Finally, 1% of RBC solutions (v/v) were prepared in PBS. Each pooled RBC sample was obtained by mixing the same group together in equal volume and adjusted to 1% RBCs (v/v).

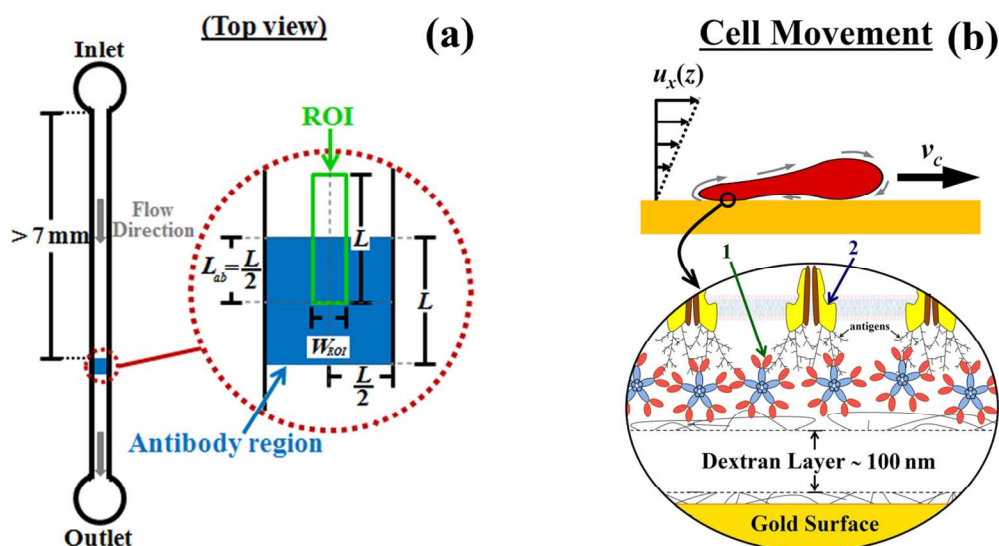


Fig. 1. Experimental setup. (a) Position of the antibody region and region of interest (ROI). In all experiments, the antibody spot is a square, where $L \approx 493 \mu\text{m}$. The RBC movement was investigated within the ROI, where the W_{ROI} is about $130 \mu\text{m}$. The ROI possesses half of the antibody region ($L_{ab} \approx 246.5 \mu\text{m}$, vertical direction). (b) The RBC movement under shear flow. The antibodies were immobilized on the carboxylated-dextran matrix, whose thickness was about 100 nm . The antigen branch is located on protein band 3, indicated by “2”. “1” indicates the antigen–antibody binding that mediates the RBC adhesion. The RBC membrane rolls up in a tank-treading motion with v_c .

Procedure of antibody immobilization and making a spot of antibody surface

The carboxylated-dextran surface was employed.²² Antibody immobilization via amine coupling was done by converting the carboxyl group to the reactive ester group with 0.4 M of EDC and 0.1 M of NHS for 10 minutes. Anti-A and anti-B antibodies in sodium acetate buffer at pH 5.5 were immediately injected for 10 minutes and an increase in the SPR signal was observed. The residual of the unreactive ester group was deactivated by reacting it with ethanolamine at pH 8.5 for 10 minutes. Unbound antibodies were washed twice with 10 mM of NaOH for 1 minute. PBS was used as a running buffer. Finally, the antibody surface was preserved by the immunoassay stabilizer in dried phase. An antibody spot was made by rotating the immobilized antibody substrate by 90° , yielding the $493 \mu\text{m} \times 493 \mu\text{m}$ spots of the antibody surface. The antibody surface density (molecules/ cm^2) can be calculated from the SPR signal.²³

A simple model of cell movement response

The relative SPR signal (RS) is defined as the ratio of the SPR signal at any time to the SPR signal of cell attachment (before the cell starts its movement). A change in the RS indicates loss of the cell from the surface. Because the detection range of the SPR sensor chip is about $200\text{--}250 \text{ nm}$, the observed RS originates from the cell membrane and some part of the inner cell or cell–surface contact area.⁸ Under a shear flow, the WSS induces RBC deformation and the RBC lifts away from the surface, depending on the WSS’s magnitude.²⁴ However, there is no further deformation or change in the cell–surface distance of a deformed RBC at a static WSS. Thus, the RS obtained from the SPR can represent the ratio of cells remaining on

the surface to the amount of adherent cells at the initial time, which is known as the adherent cell fraction.

In this experiment, a spot of antibody surface with dimensions of $L \times L$ was employed. A simple model of cell movement response is based on the assumption that the cells initially attach on the surface with uniform distribution. The cell–surface contact area or RS decreased when the cells were forced out of this spot in the direction of the fluid flow. The average cell velocity (v_c) corresponds to the rate of reduction of the RS (Section 1 of the Supplementary Information), given by

$$\frac{dRS}{dt} = -\frac{1}{L_{ab}} \sum_i w_i v_i, \quad (1a)$$

or

$$\frac{dRS}{dt} = -\frac{1}{L_{ab}} v_c, \quad (1b)$$

where w_i is the weight of the amount of adherent cells moving with cell velocity v_i . L_{ab} represents the length of the interception between the immobilized antibody region and the region of interest (ROI) as shown in Fig. 1a. Equation (1) represents the simple model of cell movement response. The relationship exhibits the linearity between v_c and time derivatives of the RS (dRS/dt).

SPR imaging instruments

The SPR imaging instrument, based on the Kretschmann configuration, was reported previously by Hounghang *et al.*¹² A tungsten-halogen lamp (Ocean optics, HL-2000-FHSA-HP, 20 W) was used as the wavelength-tunable light source, tuned from 650 nm to 900 nm by a linear variable band pass filter (Edmund Optics,

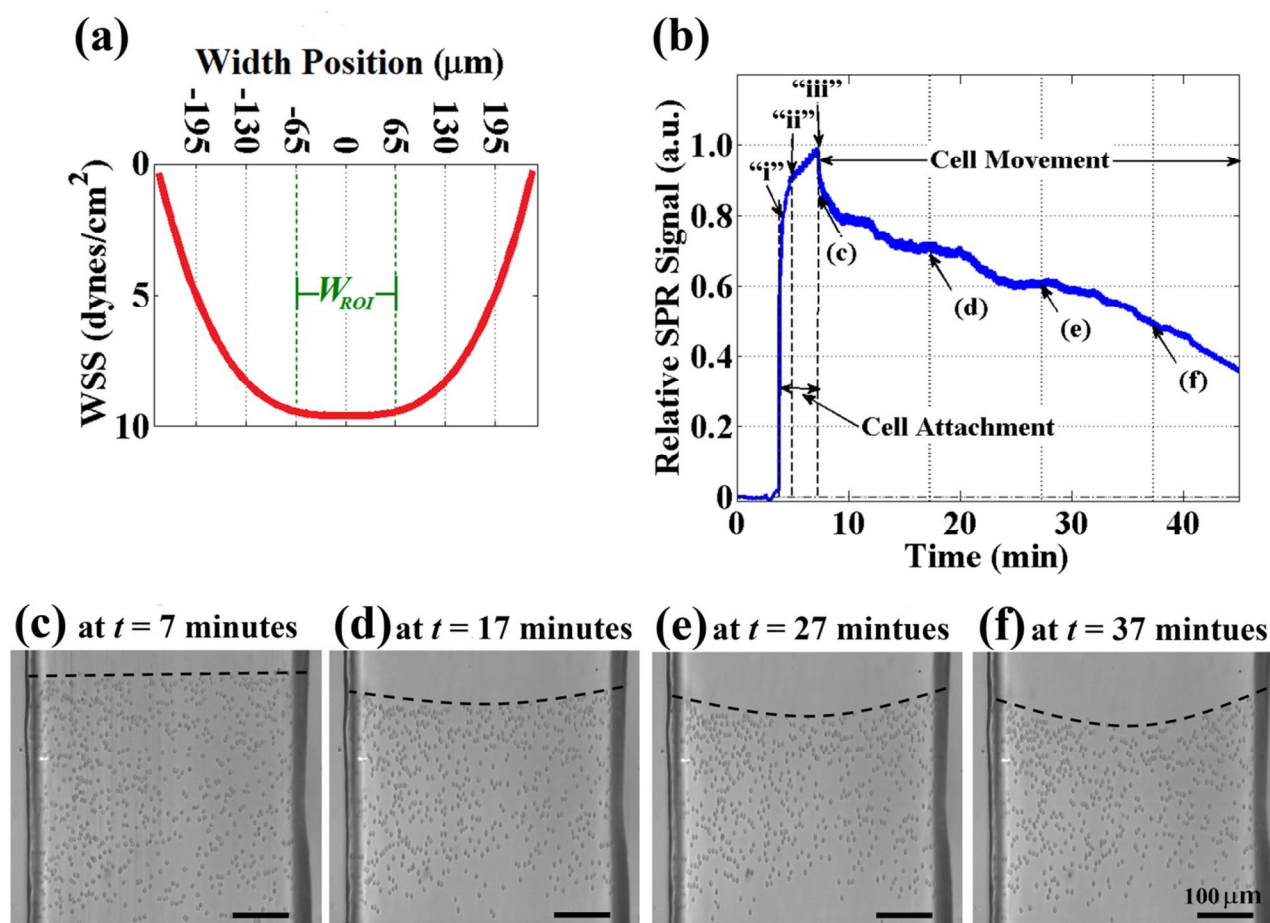


Fig. 2. Characteristics of cell movement under WSS. (a) The WSS profile of a $235 \times 496 \mu\text{m}^2$ rectangular channel, where the positions at $\pm 246.5 \mu\text{m}$ are the channel wall. The W_{ROI} occupied the position from $-65 \mu\text{m}$ to $65 \mu\text{m}$. (b) The RS during the RBC attachment and movement process. B RBCs were analyzed on the anti-B surface, which has a surface density of 6.83×10^{10} molecules/ cm^2 . "i", "ii", and "iii" indicate average WSSs within the W_{ROI} of 0, 1.92, and 9.59 dynes/ cm^2 , respectively. The RS decreases monotonically as the reduction of the adherent RBCs within the ROI as shown in images (c)–(f); the length of the scale bar is $100 \mu\text{m}$.

NT63-450). The p-polarized light was derived from a linear polarizer, collimated and illuminated to the glass prism at a fixed incident angle. The SPR sensor chip (Xantec, CMD200) was attached on the glass prism surface, connected together by an index matching gel (Cargille Labs.). The surface of a PDMS flow cell was treated with 0.05% (w/v) Pluronic F-127 for 12 hrs prior to apply onto the sensor surface by using a mechanical clamp. The buffers and samples were pumped into the flow cell by using a multi-channel peristaltic pump (Ismatec). The reflected light from the SPR chip were detected by a CCD camera (Basler, SCOUT scA1400-17gm) allowing to spatially generating the SPR curve. The wavelength was adjusted in a linear region of the SPR curve and fixed at a constant that provides the highest image contrast throughout the experiment. In-house software based on Labview was used for motion control and data processing. The cell adhesion phenomena were measured via the change of the reflected intensity, which was converted to refractive index units (RIU) by calibrating to known refractive index solutions (glycerol solution). A pixel of the SPR image was calibrated with the real length scale from circles with known diameter. The average length per pixel was found $\sim 22 \mu\text{m}$.

With the same fluidic setup of the SPR instrument, an optical microscope (Olympus, CH30) was used for the cell imaging. A top view image of cell adhesion on the sensor surface was captured through a $10\times$ objective lens collimating the light to a USB CCD camera (HDCE-20 series digital camera, BST Co., China).

Setup of wall shear stress

An illustration of an RBC adhering on an antibody surface is shown in Fig. 1b. The A and/or B antigen branches on the RBC membrane bind to the antibodies on the sensor surface. Under the shear flow, the adherent RBCs were subjected to a WSS, leading to RBC deformation and movement in the flow direction. The bond detachment occurs on the upstream (left) side of the peripheral zone of the cell–surface contact due to fluid torque. Consequently, the cell membrane rolls up like tape peeling¹⁸ and the bond rebinds on the downstream (right) side of the peripheral zone, leading to a rolling movement. The strength of the RBC adhesion is related directly to v_s , which depends on the affinity between antigen and antibody, the antibody density on the sensor surface, the antigen density on the RBC membrane, and the WSS.²⁵

All experimental processes were under a laminar flow with a calculated Reynolds number (Re) of approximately 50 for a given maximum flow rate of our pressure driven pump (flow rate $\sim 1000 \mu\text{L}/\text{min}$), where the dynamic viscosity of PBS is approximately $0.01 \text{ dynes}/\text{s}/\text{cm}^2$ ($1 \text{ dynes}/\text{cm}^2 = 0.1 \text{ Pa}$). The height and width of the rectangular channel were 235 and $493 \mu\text{m}$, respectively. To make sure that the laminar flow was fully developed, we also set the position of the ROI at over 7 mm and there was no interruption due to the RBC adhesion (the effect of a rough surface) in our experiment conditions (Detailed in Section 2 of the Supplementary Information).

The WSS profile of our rectangular channel related to the gradient of fluid velocity is like parabola as shown in Fig. 2a (the formula shown in Section 2 of the Supplementary Information). To remove analysis error from non-uniform WSS near the channel wall, an ROI with a width (W_{ROI}) of approximately $130 \mu\text{m}$ was set at the center of the antibody region. The length of the ROI was set equal to the length of the antibody spot ($493 \mu\text{m}$). The horizontal center line of the ROI overlapped the edge of the antibody region to define L_{ab} accurately (Fig. 1a). Therefore, L_{ab} from the SPR image is approximately $246.5 \pm 22 \mu\text{m}$ ($\pm 1 \text{ pixel}$). The average WSS in the ROI was calculated as a function of the flow rate. For example, a flow rate of $50 \mu\text{L}/\text{min}$ provides a WSS of approximately $2.40 \text{ dynes}/\text{cm}^2$.

Results and discussion

SPR signal of cell movement under wall shear stresses

To accurately predict v_c via the simple model of movement response (Eq. (1b)), the RBCs should adhere uniformly on the surface. Unfortunately, a non-uniform distribution results from the inertia forces, including lift²⁴ and centrifugal force,²⁶ acting on suspended RBCs which are concentrated in particular positions during flow in a microchannel. The effect of lift force can be reduced if Re is kept below 10.²⁷ The overlapping and crashing of RBCs due to the cell-velocity distribution must be considered. The amount of adherent RBCs was decreased to prevent interruption of the RBC movement along the surface while giving a satisfactory SPR signal. Figure 2b shows an example of the characteristics of the RS during the cell attachment and movement process. The cell attachment process was carried out by injecting 1% RBC solution with $Re \sim 9$ (which is low enough for the migration due to inertia to be ignored). Once the RBCs reached the sensor surface, the flow was stopped to avoid the lift force against the RBCs transporting to the surface. The RBCs were allowed to react for 1 minute before the WSS of $1.92 \text{ dynes}/\text{cm}^2$ was applied to remove the suspended RBCs from the surface for 3 minutes, since this magnitude only reduced the adhesion efficiency to 10% and was not enough to move the adherent RBCs. In all our experimental conditions, the WSS for starting the movement of the adherent RBCs was found to be between 2.40 and $4.79 \text{ dynes}/\text{cm}^2$. Therefore, the WSS of $1.92 \text{ dynes}/\text{cm}^2$ did not interrupt the cell movement analysis. Now, the adherent RBCs adhered uniformly, as evidenced by optical microscopy (Fig. 2c). The specific binding of RBCs on the antibody surface was found to be $4268 \pm 426 \text{ cells}/\text{mm}^2$. The average distance

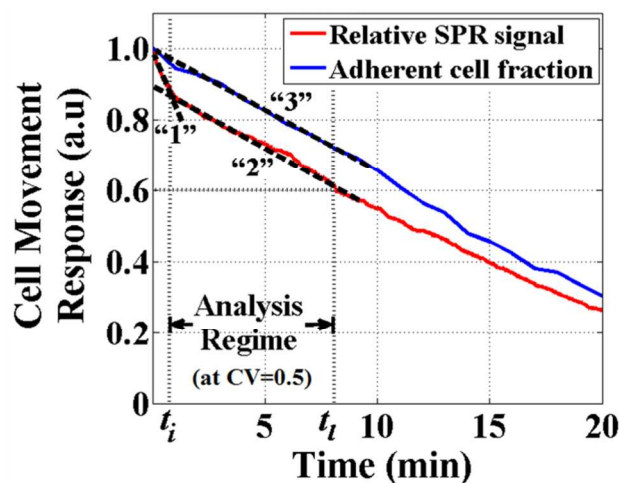


Fig. 3. The selection of the analysis regime. (a) The cell movement response, i.e., the relative SPR signal (RS) and the adherent cell fraction obtained from the SPR and the optical microscope, respectively, at a given WSS of $19.2 \text{ dynes}/\text{cm}^2$. The RS changes its behavior after a few minutes, as indicated by the dashed lines “1” (the first regime) and “2” (the second regime), where the line for each regime was found by drawing a straight line mostly going through data points of the cell movement response. The analysis regime was defined between t_i and t_f . t_i is a time point, defined as the interception point between the dashed lines “1” and “2”. t_i can be found from the coefficient of variation (CV) of the cell velocity distribution. If $CV = 0.5$, t_i corresponds to an RS of 0.6. For the adherent cell fraction, it had only one regime (the dashed line “3”). The calculated slopes of RS and the FS were -0.0348 (dashed line “2”) and -0.0342 min^{-1} (dashed line “3”), respectively.

between the adherent RBCs was approximately $8 \mu\text{m}$, which is sufficient to reduce crashing among them in our analysis time. The non-specific binding of A RBCs on anti-B surfaces and B RBCs on anti-A surfaces was tested and found to be approximately $165 \pm 57 \text{ cells}/\text{mm}^2$. All RBCs with non-specific binding can be removed by a WSS of at least $2.40 \text{ dynes}/\text{cm}^2$.

The cell movement process was carried out by adjusting the WSS to be above $2.40 \text{ dynes}/\text{cm}^2$. For an example, after the RS was saturated during the cell attachment process (Fig. 2b), the WSS at $9.59 \text{ dynes}/\text{cm}^2$ was applied. The RS decreased monotonically due to the reduction of RBCs in the ROI (Fig. 2c–2f). The edge of the area occupied by the adherent RBCs appeared as a parabolic-like profile after a long time period similar to the WSS profile. Figure 3 shows the characteristics of the adherent cell fraction and the RS. Originally, the adherent cell fraction was thought to show only one regime. However, the RS revealed that in fact two major regimes could be observed during the movement. The first regime of the RS decreased nonlinearly and more rapidly than the second regime, where the crossover time (t_i) was defined as the time point at which the first regime changed to the second regime. The aspect of two regimes caused the antibody surface density to be lower in the lateral zone of the antibody region than in the central zone (Section 3 of the Supplementary Information). The adherent RBCs near the edge of the antibody region moved

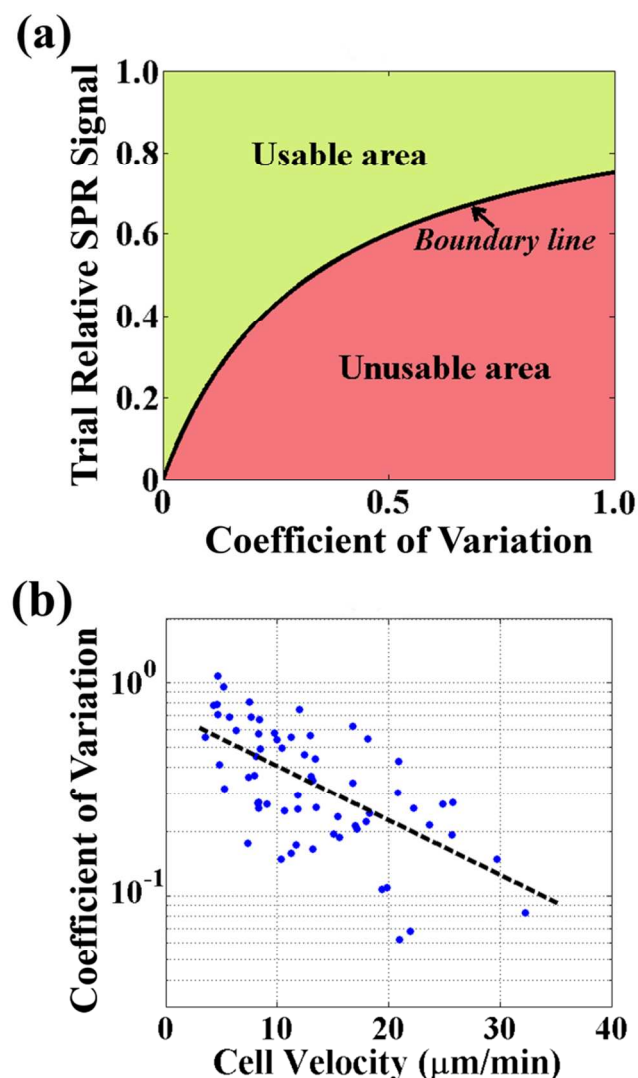


Fig. 4. (a) Diagram for choosing an available analysis regime. The analysis regime must be subject to the coefficient of variation (CV) and the trial relative SPR signal (the trial RS) staying in the usable area. (b) The precision as a function of v_c was investigated via CV.

with higher velocity than those near the center, leading to more crashing and overlapping of RBCs. This resulted in loss of the cell-surface contact area, which was observed as a steeper drop of the first regime. This was not observed in the adherent cell fraction that was obtained by the direct cell imaging or cell counting method. This situation lasted until the adherent RBCs passed from the lateral zone ($x < 70 \mu\text{m}$ from the edge) to the near-center zone ($100 \mu\text{m} < x < 246 \mu\text{m}$ from the edge), where the immobilized antibody is more uniformly distributed. The cell movement reached a constant value of v_c , leading to linearity of the second regime.

Relative SPR signal versus cell velocity

To verify the validity of the movement response model (Eq. (1b)) that is used to convert the RS to v_c , $-d\text{RS}/dt$ and v_c under the same experimental conditions were plotted as y and x, respectively.

Because they have the linear relationship, the calculated slope must be inversely proportional to the true value of L_{ab} , which is $246.5 \mu\text{m}$. The value of v_c obtained by varying the WSSs was calculated by tracking the individual RBC positions, averaging around 40 cells at any time from snapshot images during the cell movement process. A pixel of the optical microscope image was calibrated to dot images from a calibration slide (Motic). The RSs were obtained from a separate experiment but using the same fluidic setup, WSS, sample, and antibody surface density. Experimental replication was carried out at least twice (in duplicate) by using 5.0 mM of NaOH for regenerating the antibody surface, which did not diminish the binding ability of the immobilized antibody (Detailed in Section 4 of the Supplementary Information).

As mentioned above, the first regime of the RS was not taken into consideration due to the interruption of overlapping of RBCs in the lateral zone. Therefore, only the second regime was considered. Additionally, the last time period of the RS was ignored because the adherent RBCs moving with high velocity had already moved out of the ROI before others moving with low velocity. Thus, the value of RS did not represent the average information of the cell population after a long time period. This error can be avoided by choosing an analysis regime which does not exceed the limited time (t_i) that is spent to allow a group of the adherent RBCs with the highest velocity moving out of the ROI. The analysis regime was defined as the time period between t_i and t_f . However, it is easy to determine the analysis regime via a value of the RS from $\text{RS}(t_i)$ to $\text{RS}(t_f)$. Based on a normal distribution of v_i , we proposed that $\text{RS}(t_i)$ is a function of the coefficient of variation (CV) of v_i (Section 1 of the Supplementary Information).

$$\text{RS}(t_i) = 1 - \frac{1}{1 + 3\text{CV}} \quad (6)$$

Figure 4a shows a diagram for choosing the analysis regime. A reliable v_c must be under the constraint of a pair of a CV and a trial RS placed in the usable area which is the trial $\text{RS} > \text{RS}(t_i)$. To find an available analysis regime, the trial RS was chosen. Then, v_c was calculated from the range between $\text{RS}(t_i)$ and the trial RS. Finally, the trial RS and the CV calculated from the replication of v_c were checked by using the diagram (Fig. 4a). If the trial RS and the CV stayed in the usable area, the value of v_c from this analysis regime was accepted. If they stayed in the unusable area, we had to search for a new trial RS. Although this procedure seems uncomfortable, practically, it is easy to obtain the available trial RS in the first time by choosing it at almost the last point of the linear behavior of the second regime.

By using this procedure, the CV as a function of v_c was investigated. It was found that the higher the value of v_c , the lower the CV, varied from 1 to 0.1 (Fig. 4b), as well as almost independent from the length of the analysis regime. It means that the analysis regime increase for more values of the v_c . Therefore, it is better if we optimize the antibody surface density and the WSS to provide high v_c . Moreover, this is also valuable to achieve fairly good precision of the measurement ($\text{CV} < 0.2$) which is in the range of v_c from approximately 20 to

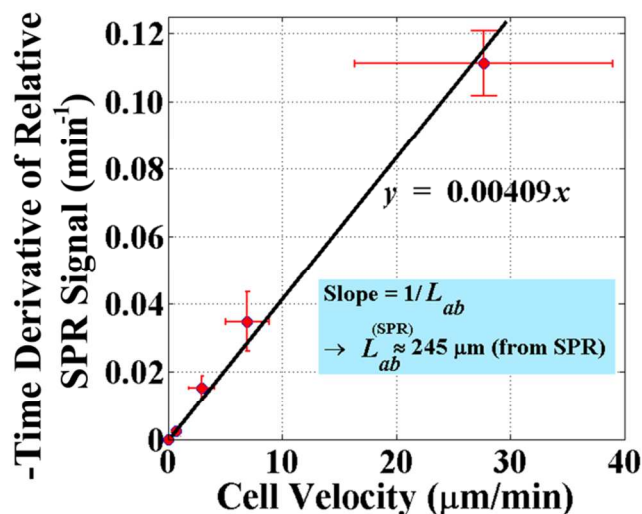


Fig. 5. The validity of the simple model (Eq. (1b)) was checked by comparing the calculated L_{ab} , which is equal to $1/\text{slope}$. The calculated L_{ab} , 245 μm , is very close to the true L_{ab} , 246.5 μm .

30 $\mu\text{m}/\text{min}$. However, high v_c provide a steep slope of the RS affecting to accuracy of the v_c calculation (detailed in next section). To solve this problem, the sensitivity of the RS to the v_c have to decrease by increasing a magnitude of L_{ab} .

To correlate v_c and $-dRS/dt$, care must be taken to ensure that v_c is observed during the same period as the RS. At a given antibody surface density, v_c increased from 0.680 to 27.7 $\mu\text{m}/\text{min}$ when WSS increased from 2.40 to 38.4 dynes/cm^2 . The available analysis regime was found by the method mentioned above. By plotting $-dRS/dt$ versus v_c , the L_{ab} calculated from the RSs is approximately 245 μm (Fig. 5), which is very close to the true L_{ab} , 246.5 μm . Although the drop of the first regime caused the error in the calculation of v_c , its effect was so insignificant that it was not found in the measurement. This suggests that our simple model is valid. It means that Eq. (1b) can be used for converting RS to v_c , which can be calculated from the second regime.

The relationship between the cell velocity and the agglutination strength

The quantitative analysis of the agglutination strength by using a flow-induced cell movement assay was carried out by observing the relationship between samples' known agglutination strengths and their v_c calculated from the RS. Higher agglutination strength should correspond to lower values of v_c . In this study, samples of subgroup A₃, subgroup B₃ (1+ to 3+ agglutination strength, corresponding to low antigen density), and subgroup A₁ and B (4+ agglutination strength) were employed. It is necessary to optimize the antibody surface density matching the WSS to obtain the available v_c satisfying every level of agglutination strength within a reasonable detection time (about 10 minutes). Namely, the second regime was not observable from the steeper RS. This means that the WSS was too high or the antibody surface density was too low. On the contrary, the RS with shallower incline required a longer period to give more reliable data (the v_c). It means that the RS(t_i) should be nearly at the boundary line (Fig. 4a). However, the value of v_c

calculated from RS can be generated in a limited range from approximately 0 to 40 $\mu\text{m}/\text{min}$ due to the limitation of our experimental setup such as size and location of the ROI, the WSS and the antibody surface density.

The v_c was correlated with the agglutination strength for both group A and group B, (Fig. 6). Lines "1" and "2" represent analysis on the anti-A regions which had different surface densities and WSSs. Line "3" represents analysis on the anti-B region. The v_c decreased monotonically with increasing agglutination strength, and this was fitted well by linear regression. As results, the line "1" and "2" have different slopes. This verified that the sensitivity of the measurement based on the flow-induced cell detachment assay can be adjusted by optimizing the antibody surface density and the WSS. Moreover, the sensitivity of line "2" is lower than that of line "3", even though the antibody surface density of anti-A is slightly less than that of anti-B. This is caused by the following: 1) the antigen density on A RBCs is twice as high as that on B RBCs,²⁸ and/or 2) the antigen-antibody affinity of group A may be better than that of group B.

Capability of distinguishing different antigen densities

To exemplify a capability of this assay for monitoring the antigen density, the v_c values of the RBCs which have slight differences in antigen density, that is, A₁ or B versus A₁B, were investigated. A₁ antigen has a higher density on A₁ RBCs ($0.81\text{--}1.17 \times 10^6$ sites per cell) than on A₁B RBC ($0.46\text{--}0.85 \times 10^6$ sites per cell), and B antigen has a higher density on B RBCs ($0.61\text{--}0.83 \times 10^6$ sites per cell) than on A₁B RBCs (0.31--

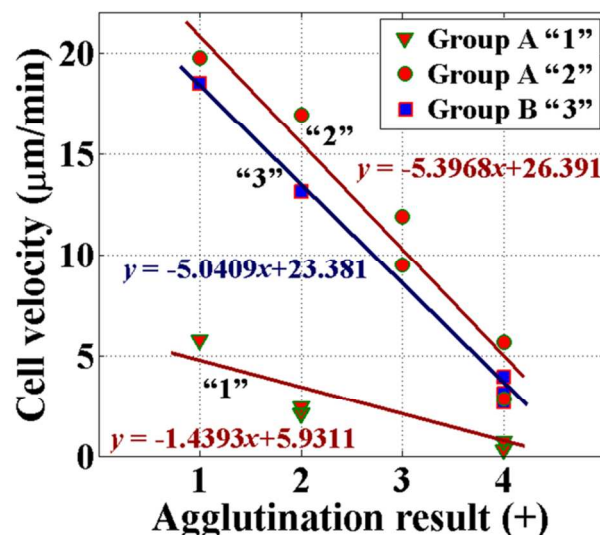


Fig. 6. The relationship between the agglutination strength and the v_c of groups A and B RBCs was investigated. This relationship can be fitted well by linear regression, where their sensitivities depend on the WSS and the antibody surface density. The conditions are: "1": WSS = 9.59 dynes/cm^2 and anti-A surface density = 6.45×10^{10} molecules/ cm^2 ; "2": WSS = 2.64 dynes/cm^2 and anti-A surface density = 3.47×10^{10} molecules/ cm^2 ; "3": WSS = 9.59 dynes/cm^2 and anti-B surface density = 6.61×10^{10} molecules/ cm^2 .

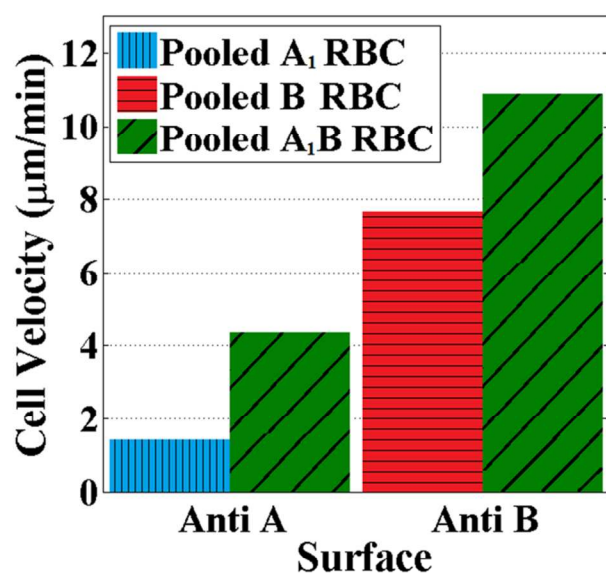


Fig. 7. The identification of slightly different antigen densities of A₁ and B versus A₁B RBC by flow-induced cell movement assay.

0.56×10^6 sites per cell).²⁸ At an WSS of 9.59 dynes/cm², pooled A₁, B, and A₁B RBCs (10 pooled samples) were analyzed on anti-A and anti-B with surface densities of 5.23×10^{10} and 5.16×10^{10} molecules/cm², respectively. The results were examined by independent two sample t-test. The difference between the v_c of A₁ and A₁B RBCs and between the v_c of B RBCs and A₁B RBCs was statistically significant ($p = 0.016$ and $p = 0.049$, respectively) at the 95% confidence interval. A₁ and B RBCs moved with lower v_c than A₁B RBCs due to higher antigen density, which allowed more formation of antigen–antibody binding (Fig. 7). This assay can distinguish the different antigen densities even though their agglutination strengths are the same (4+). The resolution of this assay, controlled by the antibody surface density and the WSS, is better than that of the agglutination technique.

Conclusions

The development of the SPR technique for the analysis of the agglutination strength based on flow-induced cell movement assay was reported. By applying the WSS to the RBCs adhering on the surface on which the specific antibody was immobilized, the agglutination strength was evaluated through the v_c of adherent RBCs rolling out of the ROI. Based on the resistance of the cell movement due to the antibody holding the antigen on the RBC membrane, a higher v_c indicated lower agglutination strength, corresponding to lower antigen–antibody bonding, and the converse. The agglutination strength was derived from v_c , which was calculated from the change in the SPR signal as a function of time. The assay can be used to quantitatively analyze the different agglutination strengths ranging from 4+ to 1+ with CV down to 0.1 depending upon v_c . We expect this work to complement the capability of the SPR technique for

cellular study. Moreover, other techniques based on solid phase support can be applied to the analysis of cell adhesion strength by using this assay.

Acknowledgements

This research was partially supported by the National Nanotechnology Center (NANOTEC), NSTDA, Ministry of Science and Technology, Thailand. K.S. was supported by the full scholarship from the Development and Promotion of Science and Technology Talents Project.

References

1. G. Daniels, *Human blood groups*, John Wiley & Sons, 2013.
2. G. Daniels and I. Bromilow, *Essential Guide to Blood Groups*, Wiley Online Library, 2014.
3. M. E. Brecher and A. A. o. B. Banks, *Technical manual/American Association of Blood Banks*, AABB, 2005.
4. J. Homola, *Chem. Rev.*, 2008, **108**, 462-493.
5. B. P. Nelson, T. E. Grimsrud, M. R. Liles, R. M. Goodman and R. M. Corn, *Anal. Chem.*, 2000, **73**, 1-7.
6. R. Wang, M. Minunni, S. Tombelli and M. Mascini, *Biosens. Bioelectron.*, 2004, **20**, 598-605.
7. L. K. Gifford, I. E. Sendroui, R. M. Corn and A. Lupták, *J. Am. Chem. Soc.*, 2010, **132**, 9265-9267.
8. R. Méjard, H. J. Griesser and B. Thierry, *TrAC, Trends Anal. Chem.*, 2014, **53**, 178-186.
9. J. M. Rice, L. J. Stern, E. F. Guignon, D. A. Lawrence and M. A. Lynes, *Biosens. Bioelectron.*, 2012, **31**, 264-269.
10. G. Steiner, *Anal Bioanal Chem*, 2004, **379**, 328-331.
11. J. G. Quinn, R. O'Kennedy, M. Smyth, J. Moulds and T. Frame, *J. Immunol. Meth.*, 1997, **206**, 87-96.
12. N. Hounkhamhang, A. Vongsakulyanon, P. Peungthum, K. Sudprasert, P. Kitpoka, M. Kunakorn, B. Sutapun, R. Amarit, A. Somboonkaew and T. Srihirin, *Sensors*, 2013, **13**, 11913-11922.
13. H. Lu, L. Y. Koo, W. M. Wang, D. A. Lauffenburger, L. G. Griffith and K. F. Jensen, *Anal. Chem.*, 2004, **76**, 5257-5264.
14. L. Weiss, *Exp. Cell. Res.*, 1961, **25**, 504-517.
15. Y. Xiao and G. A. Truskey, *Biophys. J.*, 1996, **71**, 2869-2884.
16. M. Mercier-Bonin, K. Ouazzani, P. Schmitz and S. Lorthois, *J. Colloid Interface Sci.*, 2004, **271**, 342-350.
17. B. M. Cooke, A. R. Berendt, A. G. Craig, J. MacGregor, C. I. Newbold and G. B. Nash, *Br. J. Haematol.*, 1994, **87**, 162-170.
18. M. Dembo, D. Torney, K. Saxman and D. Hammer, *Proc. R. Soc. London, Ser. B Biol. Sci.*, 1988, **234**, 55-83.
19. D. A. Hammer and S. M. Apte, *Biophys. J.*, 1992, **63**, 35-57.
20. D. K. Brunk and D. A. Hammer, *Biophys. J.*, 1997, **72**, 2820-2833.
21. W. Malomgré and B. Neumeister, *Anal Bioanal Chem*, 2009, **393**, 1443-1451.
22. S. Lofas, *Pure Appl. Chem.*, 1995, **67**, 829-834.
23. L. S. Jung, C. T. Campbell, T. M. Chinowsky, M. N. Mar and S. S. Yee, *Langmuir*, 1998, **14**, 5636-5648.

Analyst

- 1 24. D. Di Carlo, *Lab Chip*, 2009, **9**, 3038-3046.
- 2 25. C. Dong and X. X. Lei, *J. Biomech.*, 2000, **33**, 35-43.
- 3 26. R. Burger, D. Kirby, M. Glynn, C. Nwankire, M. O'Sullivan, J.
- 4 Siegrist, D. Kinahan, G. Aguirre, G. Kijanka, R. A. Gorkin Iii
- 5 and J. Ducreé, *Curr. Opin. Chem. Biol.*, 2012, **16**, 409-414.
- 6 27. A. A. S. Bhagat, H. W. Hou, L. D. Li, C. T. Lim and J. Han, *Lab*
- 7 *Chip*, 2011, **11**, 1870-1878.
- 8 28. J. Economidou, N. Hughes-Jones and B. Gardner, *Vox Sang.*,
- 9 1967, **12**, 321-328.
- 10
- 11
- 12
- 13
- 14
- 15
- 16
- 17
- 18
- 19
- 20
- 21
- 22
- 23
- 24
- 25
- 26
- 27
- 28
- 29
- 30
- 31
- 32
- 33
- 34
- 35
- 36
- 37
- 38
- 39
- 40
- 41
- 42
- 43
- 44
- 45
- 46
- 47
- 48
- 49
- 50
- 51
- 52
- 53
- 54
- 55
- 56
- 57
- 58
- 59
- 60

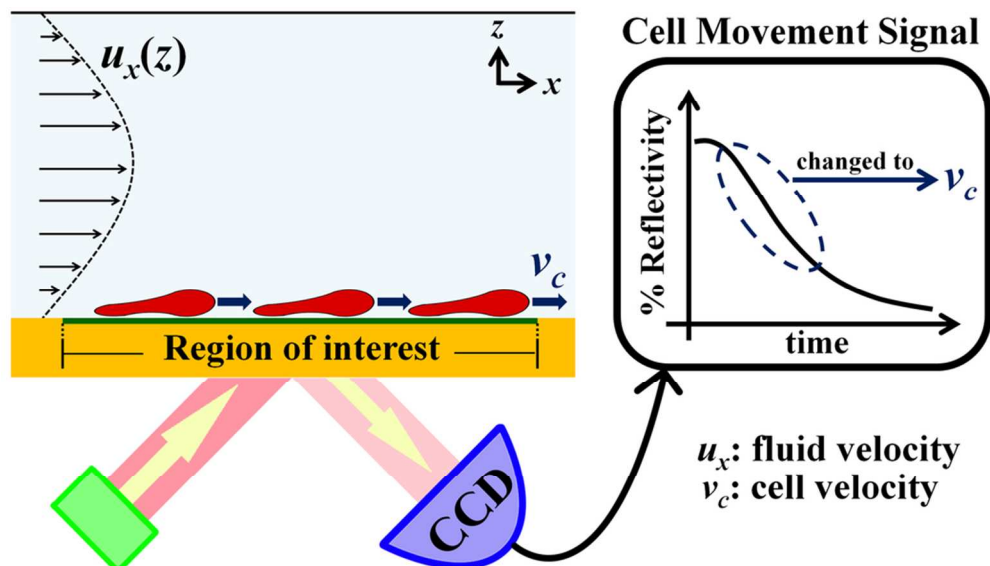


Illustration of the flow-induced cell movement assay. a flow-induced cell movement assay is developed as a tool for the quantification of the strength of RBC agglutination or the cell-surface adhesion. The assay is done by monitoring the movement of the RBC interacted with the immobilized antibody via the SPR intensity changed. The speed of the RBC movement can be calculated and is related to the agglutination strength.

44x25mm (600 x 600 DPI)